The pH in the Microenvironment of Human Mesenchymal Stem Cells Is a Critical Factor for Optimal Osteogenesis in Tissue-Engineered Constructs

To cite this article:
Monfoulet Laurent-Emmanuel, Becquart Pierre, Marchat David, Vandamme Katleen, Bourguignon Marianne, Pacard Elodie, Viateau Véronique, Petite Herve, and Logeart-Avramoglou Delphine. Tissue Engineering Part A. July 2014, 20(13-14): 1827-1840. doi:10.1089/ten.tea.2013.0500.

Published in Volume: 20 Issue 13-14: July 10, 2014
Online Ahead of Print: February 24, 2014
Online Ahead of Editing: January 21, 2014

Author information

Laurent-Emmanuel Monfoulet, PhD,[1] Pierre Becquart, MS,[1] David Marchat, PhD,[2] Katleen Vandamme, PhD, MDD,[1,3] Marianne Bourguignon, MS,[1] Elodie Pacard, PhD,[4] Véronique Viateau, DVM, PhD,[1,5] Herve Petite, PhD,[1] and Delphine Logeart-Avramoglou, PhD[1]

[1]Laboratory of Bioengineering and Bioimaging for Osteo-Articular Tissues, UMR 7052 CNRS, Université Paris Diderot, Sorbonne Paris Cité, Paris, France.

[2]Center for Health Engineering, Ecole Nationale Supérieure des Mines de Saint-Etienne, Saint-Etienne cedex 2, France.

[3]Department of Oral Health Sciences and Dental Clinic, BIOMAT, KU Leuven, University Hospitals Leuven, Leuven, Belgium.

[4]NORAKER, Villeurbanne, France.

[5]National Veterinary School of Alfort, Paris-Est University, Maisons-Alfort, France.

Address correspondence to:

Delphine Logeart-Avramoglou, PhD

Laboratory of Bioengineering and Bioimaging for Bone and Articulations

UMR 7052 CNRS

Université Paris Diderot

Sorbonne Paris Cité

10 avenue de Verdun

75010 Paris

France
E-mail: delphine.logeart@univ-paris-diderot.fr

Received: August 13, 2013
Accepted: January 6, 2014

ABSTRACT

The present study aimed at elucidating the effect of local pH in the extracellular microenvironment of tissue-engineered (TE) constructs on bone cell functions pertinent to new tissue formation. To this aim, we evaluated the osteogenicity process associated with bone constructs prepared from human Bone marrow-derived mesenchymal stem cells (hBMSC) combined with 45S5 bioactive glass (BG), a material that induces alkalinization of the external medium. The pH measured in cell-containing BG constructs was around 8.0, that is, 0.5 U more alkaline than that in two other cell-containing materials (hydroxyapatite/tricalcium phosphate [HA/TCP] and coral) constructs tested. When implanted ectopically in mice, there was no de novo bone tissue in the BG cell-containing constructs, in contrast to results obtained with either HA/TCP or coral ceramics, which consistently promoted the formation of ectopic bone. In addition, the implanted 50:50 composites of both HA/TCP:BG and coral:BG constructs, which displayed a pH of around 7.8, promoted 20–30-fold less amount of bone tissue. Interestingly, hBMSC viability in BG constructs was not affected compared with the other two types of material constructs tested both in vitro and in vivo. Osteogenic differentiation (specifically, the alkaline phosphatase [ALP] activity and gene expression of RUNX2, ALP, and BSP) was not affected when hBMSC were maintained in moderate alkaline pH (≤7.90) external milieu in vitro, but was dramatically inhibited at higher pH values. The formation of mineralized nodules in the extracellular matrix of hBMSC was fully inhibited at alkaline (>7.54) pH values. Most importantly, there is a pH range (specifically, 7.9–8.27) at which hBMSC proliferation was not affected, but the osteogenic differentiation of these cells was inhibited. Altogether, these findings provided evidence that excessive alkalinization in the microenvironment of TE constructs (resulting, for example, from material degradation) affects adversely the osteogenic differentiation of osteoprogenitor cells.

Introduction

Bone marrow-derived mesenchymal stem cells (BMSC), which are able of osteodifferentiation and, thus, promote bone formation,1,2 support the repair and/or regeneration of osseous defects when they are distributed in appropriate biomaterial scaffolds.3–6 Such scaffolds are designed as temporary matrices for supporting new tissue development and bone growth. The ideal scaffolds should provide a framework, as well as a specific environment, for cell attachment, proliferation, differentiation, and formation of tissue-specific extracellular matrix (ECM).7 Such scaffolds should also be absorbable with rates of resorption that are commensurate to those of bone formation.

Understanding, and controlling, pertinent cell functions by modulating the local engineered extracellular environment is a critical issue in the development of suitable material scaffolds for bone tissue engineering (TE) applications. In this respect, an extensive number of studies have reported the significant effect of scaffold properties, such as chemical composition, surface topography and chemistry, pore size, porosity, and specimen size on cell functions and, therefore, on the osteogenic outcome of engineered scaffolds.8,9 However, the microenvironment or milieu where the cells reside has received little attention. This issue is even more critical because such local environments can be affected by the resorption of the scaffold material, especially by solutes arising from the material dissolution and by concomitant pH changes.10

Among the biomaterials tested for bone TE application to date, calcium-based materials, such as hydroxyapatite (HA), tricalcium phosphate (TCP), calcium carbonate (coral) ceramics, and bioactive glass (BG), are the most promising ones. These calcium-containing materials are appropriate for bone-related applications because of similarities of their chemical and mechanical properties with the mineral phase of natural bone. In addition, these materials are considered osteoconductive and

bioactive because of both their bonding capacity to surrounding osseous tissue and the ability to promote new bone tissue formation.11,12 When combined with human BMSC (hBMSC), HA, TCP, biphasic HA/TCP, and coral ceramics induced de novo bone tissue in the subcutis of immunocompromised mice.13–18 In contrast, and despite the expanding application of BG (such as 45S5 BG) and glass ceramics as bone substitutes,19 information regarding the osteogenic potential of hBMSC in combination with BG scaffolds is strikingly lacking in the bone TE field.

Whereas the biocompatibility and osteoconductivity of BG has long been established,19,20 such material is also known for the release of ion dissolution products as well as for inducing alkalinization of the external medium upon exposure to either physiological solutions or body fluids.21–23 Changes in the extracellular fluid pH of the local biological microenvironment can profoundly affect cell metabolism and function22,24 as well as the processes of bone tissue formation and mineralization.25 Chronic systemic acidosis promotes bone resorption, whereas alkalosis promotes bone formation by stimulating pertinent osteoblast functions.26–28 More recently, Shen et al. reported the beneficial role of local alkalinization mediated by borosilicate BG on the viability of preosteoblasts.10 However, the positive or negative effect of pH in cell constructs has never been investigated in the bone TE field. This aspect is crucial since the implanted hBMSC are in a confined space within tissue constructs and are, therefore, especially vulnerable to chemical changes within the local biological microenvironment.

For these reasons, the present study focused on examining the impact of pH, specifically, alkalinization, in the engineered extracellular microenvironment on hBMSC-mediated osteogenesis. To this aim, we evaluated both in vitro and in vivo, the osteogenicity of bone constructs prepared from hBMSC combined with 45S5 BG (a material that induces alkalinization of the external medium) in comparison with results obtained using two other clinically available, calcium-based scaffolds, specifically, biphasic HA/TCP and coral ceramics. Biomaterial granules of equivalent size (~400 μm in diameter), similar construct preparation, and similar implant dimensions were used to ensure an equivalent material surface area (at the cell scale) as well as an equivalent intergranule volume available to cells within three-dimensional (3D) material constructs. The in vivo osteogenic outcomes of TE constructs were correlated with their local pH. In addition, the in vitro effect of pH on the proliferative and osteogenic differentiation of hBMSC was determined.

Materials and Methods

Material scaffolds

Three calcium-based materials in the form of granules were studied. These granules differed in terms of their chemical composition as well as shape and surface area, but all had sizes in the 300–690 μm range. The biphasic calcium phosphate granules (HA/TCP), composed of 60% HA and 40% TCP, were produced using the spray drying process followed by high temperature calcination; these granules (300–570 μm; mean size: 417 μm) were donated by Zimmer, Inc. Natural coral granules (Porites species; Biocoral®) consisted of 99% calcium carbonate in the form of aragonite29,30; these materials (300–600 μm; mean size: 426 μm) were donated by Inoteb, Inc. The nonporous 45S5 silicate BG (designated BG hereafter) granules of nominal 45% SiO_2, 24.5% CaO, 24.5% Na_2O, and 6% P_2O_5 in wt% composition (300–690 μm; mean size: 457 μm) were donated by Noraker and were preconditioned in laboratory-made simulated body fluid (SBF) as recommended by the supplier. Briefly, BG granules were immersed in a SBF solution (0.1 g of BG per mL of solution) and were maintained under mild stirring by rotation at 37°C for 4 weeks. The SBF solution was renewed twice a week. Then, granules were rinsed with double distilled water and dried before sterilization. SBF

pretreatment promotes the formation of a bone-like carbonated HA (cHA) layer as well as calcite on its surface.31–34

The surface of the granules used in the present study was examined using scanning electronic microscopy (SEM) (SEM-FEG, JEOL JSM-6500F). The specific surface areas were determined according to the BET method 8 points using N2 adsorption isotherms (Micromeritics ASAP 2010) as previously described.35 The particle size distribution was determined by using a laser diffractometer with a Hydro 2000S module (Mastersizer 2000 from Malvern Instruments Ltd.).

hBMSC isolation, expansion, and labeling with Luc gene

hBMSC were harvested from bone marrow obtained as discarded tissue (intramedullary reamings) from four female patients and one male patient 17, 31, 31, 49, and 63 years old (mean age: 38.8±17.7 years) who were operated for traumatic orthopedic indications in the absence of any detected chronic pathologies (such as diabetes, cancer, arthritis) at the Lariboisiere Hospital (Paris, France). The tissues were collected with the respective patient's consent in agreement with Lariboisière Hospital (Paris, France) regulations. The hBMSC were isolated using a procedure adapted from literature reports.1 Briefly, cells were harvested by gently flushing the collected bone marrow samples through decreasing (from 16G to 21G) needle sizes. These cells were then cultured in a standard cell culture medium, that is, alpha-modified minimum essential medium (αMEM) containing 10% fetal calf serum (PAA Laboratories) and 1% of an antibiotic/antimycotic solution (PAA Laboratories), in a humidified, 37°C, 5% CO2/95% air environment. When the hBMSC reached 60–70% confluence, they were trypsinized and subcultured at a density of 1000–5000 cells cm2. HBMSC obtained from the five aforementioned patients were pooled at the same density, expanded, and used up to passage 4–5 for the experiments described in the sections that follow.

Genetically modified hBMSC were obtained following their transduction with a lentiviral vector encoding firefly luciferase (pTMLW-MND-Luc; Vector platform/INSERM U876) as previously described.36 Transduced cells (designated as LuchBMSC hereafter) were expanded and used to monitor the hBMSC viability in cell-containing constructs both in vitro and in vivo.

Preparation of cell-containing constructs

For all cell-related experiments in the present study, aliquots of 40 mg of granules of the materials tested were sterilized by autoclaving, then sequentially rinsed twice in phosphate buffer saline (PBS), and also rinsed once in a serum-free αMEM (Sigma-Aldrich) cell culture medium.

Aliquots of hBMSC (or LuchBMSC when so specified) were delivered (suspended in 100 µL of standard cell culture medium) to each material granules tested; the final cell density was 106 cells per cell-containing construct for in vivo studies or 105 cells per construct for in vitro studies. Unseeded scaffolds served as controls. After 4 h of incubation at 37°C, the supernatant was discarded and the granules were embedded in a fibrin gel (Tissucol®; Baxter) prepared by mixing 100 µL of fibrinogen (9 mg mL−1) with 5 µL of thrombin (100 UI mL−1) as previously described.37 These cell-containing constructs were maintained in 2 mL of standard cell culture medium at 37°C overnight before use in experiments.

In vivo studies

Ten-week-old, female, nude mice were obtained from Janvier and handled according to the European Guidelines for Care and Use of Laboratory Animals (EEC Directives 86/609/CEE of 24.11.1986). All experimental animal procedures conducted in the present study were approved by the Ethics Committee on Animal Research of the Lariboisiere/Villemin, Paris, France. The hBMSC-

containing constructs (n=7 per group for the HA/TCP, coral, and BG constructs; n=6 per group for both the HA/TCP-BG and coral-BG composite constructs) were subcutaneously implanted in mice as previously described.36 Briefly, each mouse was preoperatively given analgesics (0.4 mg of buprenorphine per kg animal weight; Axience), anesthetized by intraperitoneal injection of 100 mg kg−1 ketamine (Ketalar®; Virbach) and 10 mg kg−1 xylazine (Rompun® 2%; Bayer), and its skin was disinfected. Symmetrical incisions were made on the back of each mouse on both sides of the spine and subcutaneous pouches were created. The cell-containing constructs to be tested were inserted into each pouch (four constructs per mouse). The soft tissues at the implantation sites were then closed with interrupted nonresorbable sutures. Eight weeks postimplantation, the animals were sacrificed through injection of lethal doses of pentobarbital (Dolethal®; Vetoquinol). At that time, the constructs were retrieved en-bloc and fixed in 10% (v/v) phosphate-buffered formalin before analysis as described in the next section.

For monitoring the implanted cell survival in vivo, special cell-containing constructs were prepared using LuchBMSC. Following implantation of these cell constructs, the mice were imaged twice a week during the 8-week postimplantation period as previously described.38 Briefly, the mice were anesthetized by inhaling isoflurane followed by local injection of 100 µL of D-luciferin (15 mg mL−1 in PBS) at each implantation site. The animals were then imaged using a bioluminescence imaging system (Ivis Lumina II®; Caliper Life Sciences). Standard regions of interest surrounding each implant were delineated on the bioluminescence images and the photon flux emitted by each construct was quantified using the Living Image® 3.1 software (Caliper Life Science). To compare cell survival in each construct tested, photon fluxes were normalized with respect to the signal acquired at the beginning (day 1) of the respective in vivo experiment.

Histology and immunohistochemistry

Six out of seven retrieved constructs for each material tested were processed for undecalcified histology. After fixation, the explanted samples were rinsed in water, dehydrated in ethanol, cleared in xylene, and embedded in methyl methacrylate as previously described.29 Each sample was then cut into either six or seven sections (each 500 µm thick) using a diamond circular saw (Leica 1600; Leica). Each such specimen section was then grounded to a thickness of 100 µm and stained using Stevenel's blue and Van Gieson Picrofuchsin red for subsequent histological analysis. Three nonadjacent sections from each specimen were selected for histomorphometrical analysis. Histological examination was performed using an optical microscope (Nikon Eclipse TE2000-U; Nikon France) equipped with a numeric camera (DXM1200F; Nikon). Bone was quantified using the NIS-Elements BR 2.30 software (Nikon). The surface area of bone (stained in red) was measured in each specimen section and normalized over the whole surface area delineated around each section.

The remaining seventh retrieved construct (from the HA/TCP, coral, and BG construct groups) was fixed in 4% paraformaldehyde (pH 7.4) for 36 h, decalcified in Decalcifier II (Surgipath) at 4°C for 48 h, and embedded in paraffin. Sequential sections were processed for human beta-microglobulin (a membrane protein that enables tracking human cells) immunodetection. Briefly, tissue sections were pretreated in a proteolytic enzyme solution (Dako) at 37°C for 20 min. Cell membranes were permeabilized using 0.3% Triton X-100 for 15 min; the endogenous peroxidase activity was inhibited by addition of peroxidase block (Kit Envision+; Dako), and the nonspecific binding sites were blocked using Protein Block (Dako). The tissue sections thus prepared were sequentially incubated in the primary antibody, polyclonal rabbit anti-beta-2-microglobulin (1/1000; Novocastra) for 1 h, incubated with the Labelled Polymer-HRP Anti-Rabbit antibody (Envision+ Kit, K4011; Dako) for 30 min, and visualized using the DAB chromogen (Envision+ Kit, K4011; Dako) for 5 min.

In vitro hBMSC adhesion and proliferation onto material scaffolds

Cell adhesion was assessed using SEM. Briefly, hBMSC were seeded onto granules (103 cells per mg of material granules) and cultured under standard cell culture conditions for 24 h. At that time, the specimens were washed once with cacodylate 0.1 M (pH 7.4) and fixed in 2.5% glutaraldehyde (in cacodylate 0.1 M; pH7.4) at 4°C for 1 h. After two washings in cacodylate, the specimens were dehydrated in successively increasing concentrations of alcohol (from 30% to 100%). For SEM examination, the specimens of interest were treated in hexamethylsilazane baths (HMDS; Delta microscopy), dried overnight, and coated using a sputter coater equipped with a gold target (EMSCOPE SC 500; Elexience). These specimens were examined using a 505 Philips SEM (FEI Company) at 10 keV.

Proliferation of hBMSC onto the material granules tested was monitored in vitro both in two-dimensional (2D) (i.e., granules deposited on the bottom of a tissue culture polystyrene [TCPS] dish) and in 3D (i.e., granules dispersed within fibrin gel constructs). Cell proliferation in 2D conditions was determined by DNA quantification. Specifically, aliquots of 40 mg of material granules were transferred in each well of 48-well plates; hBMSC (3×104 cells) in a standard cell culture medium were seeded. At different times of culture (specifically, at 0, 14, 21, and 28 days), cells were lysed using the lysis buffer (1 mM MgCl2, 0.1 M Na2CO3, 0.1 M NaHCO3, 0.1% Triton X100 [v/v]; pH 10.2) and freeze/thawed three times (to disrupt the cell membranes). Cell DNA content was determined using the CyQuant® cell proliferation assay kit (Molecular Probes) according to the manufacturer's instructions. Cell proliferation in the 3D constructs was assessed using bioluminescent (BLI) imaging. For this purpose, the cell constructs were prepared using LuchBMSC (105 cells per construct), transferred into 24-well plates, and cultured in the standard cell culture medium for the prescribed time periods (up to 28 days). The BLI signal from each cell-containing construct was determined nondestructively three times a week by adding D-luciferin (at a final concentration of 300 ng mL−1 PBS) into each cell construct-containing well; BLI images were acquired using a bioluminescence imaging system. To compare the time course of cell proliferation in each construct tested, photon fluxes were normalized with respect to the signal acquired at the beginning (day 1) of the respective cell culture period.

Determination of the osteogenic differentiation of hBMSC in vitro

In the present study, to assess the osteogenic differentiation of hBMSC cultured onto the material granules of interest, cells were seeded at a density of 3×103 cells cm2 in each well of six-well plates in the presence of 40 mg of granules of each one of the three materials tested. These cells were cultured in the osteogenic medium, which is the standard cell culture medium containing 10−7 M dexamethasone, 150 µM ascorbic acid-2 phosphate, and 2 mM β-glycerophosphate (all chemicals from Sigma-Aldrich), for up to 28 days. The supernatant medium was replaced every 2–3 days for the duration of the study. To assess the impact of the cell culture medium pH on the osteogenic differentiation of hBMSC, the cells (3×103 cells cm2) were cultured in the osteogenic medium buffered with 25 mM 4-(2-hydroxyethyl)-1-piperazineethanesulfonic acid (HEPES) the pH adjusted at either 7.47, 7.90, 8.27, 8.85 or 9.37, and cultured in a humidified, 37°C, atmospheric air environment (in the absence of supplementary CO2 inlet) for up to 28 days. Cells in the culture medium buffered using the physiological CO2/HCO3 buffer system at pH 7.54 were the respective controls. In this experiment, the initial pH value (pHini) of the osteogenic culture medium (which was added fresh to the cells) and the final pH value (pHfin) of the supernatant cell culture medium (which was removed from the cells) were specifically checked at each culture medium change (i.e., every 2–3 days) during the cell culture period.

At the end of each prescribed cell culture period, the osteogenic differentiation of these cells was assessed by quantifying expression of a panel of osteoblastic markers (as described in the next section) as well as by determination of the activity of alkaline phosphatase (ALP) and mineralization. The ALP activity was determined both by staining the cell cultures in situ using a commercially available kit according to the manufacturer's (Sigma-Aldrich) instructions and by quantifying the ALP activity in cell lysates as previously described.39 The presence of calcium-containing deposits in the ECM was detected by staining the cells using the Alizarin red (AR) method. All these experiments were performed in triplicate and repeated at two separate times.

Quantitative gene expression analysis by real-time polymerase chain reaction

Total ribonucleic acid (RNA) was extracted from hBMSC using the NucleoSpin RNA II kit (Macherey-Nagel). The RNA concentration was measured using a NanoDrop ND-1000 (LabTech) spectrophotometer. One microgram of extracted RNA was used as template for single-strand cDNA synthesis using the SuperScriptTM II Reverse transcriptase Kit (Invitrogen). Five microliters of cDNA (diluted at a 1:20 ratio) was used to program amplifications through real-time polymerase chain reaction (PCR) using specific primers of genes encoding for runt-related transcription factor 2 (RUNX2) (Hs00231692_m1), collagen type 1 α1 (Col1a1) (Hs00164004_m1), osteopontin (OPN) (Hs00960942_m1), osteocalcin (OC) (Hs00609452_g1), and for bone sialoprotein (BSP) (Hs00173720_m1) (all from Applied Biosystems, Inc.), combined with TaqMan Universal PCR Master Mix using the MyiQ™ Single-Color Real-Time PCR thermocycler (Bio-Rad Laboratories) according to the protocol described previously.40 All samples, including specimens from experiments and standards (n=3 for each condition), were run in triplicate and in parallel. Data were analyzed using the iCycler IQ software (Biorad) and were compared by the ΔΔCt method. The results from hBMSC cultured onto the material granules tested in the present study were normalized to the amount of 18S transcript and were expressed relative to the results obtained from cells at day 0. The results from hBMSC cultured at different pH values were normalized to the amount of 18S transcript, and were expressed relative to the results obtained from hBMSC cultured in the nonosteogenic medium for the same time period.

pH in the 3D constructs

To determine the pH in the core environment of the material constructs containing the tested granules (without cells), a microelectrode (PerpHecT®ROSS; Thermo Scientific) was inserted in the material granules before the fibrin gelation. After gelation, the constructs were maintained in 2 mL of weakly buffered solution, specifically, PBS (1 mM sodium phosphate at pH 7.4) to minimize the buffering impact on the pH determination. The pH was monitored at room temperature for 24 consecutive hours. The global pH of the constructs seeded with 106 hBMSC was also determined before (day 0) and after implantation in mice for either 3 or 7 days. After animal sacrifice, the cell constructs were excised, chopped into small pieces, and transferred in 1 mL of 1 mM PBS solution (pH 7.4). After mixing, the pH of each such solution was measured using a calibrated pH meter (Star Orion).

Statistical analyses

Numerical results are reported as mean±standard deviation. The nonparametric Mann–Whitney U-test was used to analyze data from two independent conditions. When comparing data of more than two conditions, the Kruskal–Wallis one-way analysis test was used. Quantitative data from in vivo BLI signals were analyzed using the two-way analysis of variance. For all analyses, differences were considered to be statistically significant at $p<0.05$.

Results

Physical properties of the granule surfaces

Visualization of the three materials tested using SEM enabled analysis of their macro- and microstructure (Fig. 1A–F). The HA/TCP granules exhibited a round shape and rough surface texture (Fig. 1A). At higher magnification (Fig. 1B), the round HA/TCP granules contained dense aggregates (1–10 μm) of round elemental particles/grains of the 100 nm size. The shapeless aggregates, which formed agglomerates, were lightly bonded in contrast to the elemental grains that were highly sintered (i.e., more strongly bonded). The coral granules had branching shapes (Fig. 1C). At higher magnification (Fig. 1D), the coral granules exhibited a rough and granular surface as that observed with HA/TCP granules. The main coral granules were composed of dense aggregates of small, round, and acicular particles a few nanometers in size (Fig. 1D). The coral appeared denser than the HA/TCP granules (Fig 1B). The BG granules, preconditioned with SBF, displayed sharp angular shapes (Fig. 1E). At higher magnification (Fig. 1F), the cHA layer coating the surface of the BG granules contained round aggregates ranging between 200 nm and 1 μm in diameter, which were composed of smaller particles of about 100 nm in diameter. The specific surface area of the coral, HA/TCP, and BG granules was 0.06, 0.33, and 1.09 m2g−1, respectively. Altogether, these observations indicated that, at the nanometer scale, the surface topography and roughness of the three materials tested were different, but at the hBMSC scale (20–50 μm), they were similar.

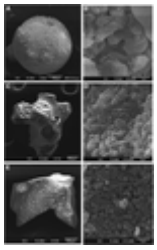

FIG. 1. Scanning electron micrographs of HA/TCP (A, B), coral (C, D), and BG (E, F) granules at low (A, C, E) and high (B, D, F) magnification. BG, bioactive glass; HA/TCP, hydroxyapatite/tricalcium phosphate.

In vivo bone formation by hBMSC contained in the constructs tested

De novo bone formation was assessed when hBMSC-containing constructs (prepared with either HA/TCP, coral, BG or composite of either HA/TCP:BG or coral:BG) were implanted ectopically in a mouse model. After 8 weeks of subcutaneous implantation, there was no bone formation in conjunction with material scaffolds without cells; these scaffolds, however, were infiltrated with fibrous tissue (data not shown). At the same time point, new bone tissue was observed both in the hBMSC-containing HA/TCP and coral constructs as shown in the representative histology results from such explants (Fig. 2A). The osteogenic outcome of hBMSC contained within the tested coral- and HA/TCP- implants was similar and was characterized by high prevalence of bone formation and by similar amount of deposited new bone tissue (Fig. 2B). In contrast, no bone tissue was detected in any of the hBMSC-containing BG constructs (Fig. 2A, B). When hBMSC were contained within the 50:50 composites of either HA/TCP:BG or coral:BG constructs, newly formed bone was found at the periphery of the constructs as well as consistently in contact with the coral and HA/TCP material surfaces. Very small amount of bone tissue (<0.2% compared with 4.2% and 3.8% for HA/TCP and coral cell-containing constructs, respectively) was observed (Fig. 2A) and the prevalence of bone formation was reduced (Fig. 2B) in composite constructs. Altogether, the present results provided

evidence that, in contrast to the HA/TCP and coral materials tested, hBMSC cultured on BG did not induce bone formation; moreover, the presence of BG in the composite constructs tested had a negative effect on osteogenesis.

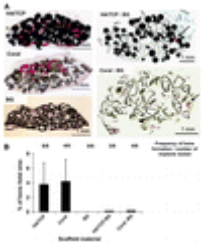

FIG. 2. Ectopic bone formation after 8 weeks of subcutaneous implantation of scaffolds containing hBMSC. (A) Representative, undecalcified, histological cross sections of hBMSC-containing constructs composed of either HA/TCP, coral, BG granules or composites of either HA/TCP:BG or coral: BG (50:50 w/w). Stains: Stevenel's blue and Van Gieson Picrofuchsin red. (B) Amount of new bone tissue determined by histomorphometric analysis. The frequency of bone formation per implant material tested is also indicated. *Material scaffold; the red color provided evidence for mineralized bone tissue. Arrows locate area of new bone formation in composites of HA/TCP or Coral:BG. hBMSC, human bone marrow-derived stromal cells. Color images available online at www.liebertpub.com/tea

Viability of hBMSC onto the materials tested

The issue of potential toxicity of BG on hBMSC was addressed. For this purpose, adhesion and proliferation of hBMSC on the material granules was determined. SEM examination at 24 h confirmed that the hBMSC adhered and spread in a similar fashion onto the three substrates tested (Fig. 3A). Cell proliferation was determined when hBMSC were cultured onto granules of each one of the three materials tested that had been placed on the bottom of individual wells of tissue culture dishes (Fig. 3B). DNA quantification at different time points over a 4-week period of culture provided evidence that, under these conditions, hBMSC proliferation was similar for hBMSC cultured on the three materials tested as well as on TCPS, the reference substrate (Fig. 3B).

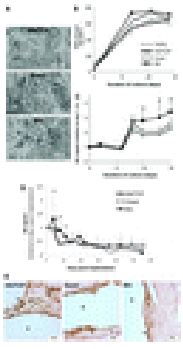

FIG. 3. Viability of hBMSC onto material scaffolds either cultured in vitro (A–C) or implanted in vivo in nude mice (D, E). (A) In vitro hBMSC adhesion evaluated by scanning electronic microscopy 24 h postcell seeding. (B) In vitro cell proliferation assessed when hBMSC were cultured either directly on tissue culture polystyrene (TCPS; TPP®) alone or onto granules placed on the bottom of individual wells of TCPS dishes and determined by DNA quantification; (C) In vitro cell proliferation assessed when LuchBMSC were cultured within three-dimensional constructs (composed of material granules

embedded in fibrin gel) and determined by BLI monitoring. Photon fluxes (normalized to those obtained at day 1 after cell seeding) were plotted versus the number of days of cell culture. $p<0.001$ (two-way analysis of variance [ANOVA]); #$p<0.05$ for the BG constructs compared with the other two material constructs tested (Mann–Whitney test). (D) In vivo cell viability was determined by monitoring BLI over 58 days of implantation: photon fluxes (normalized to those obtained at day 1 postimplantation) were plotted versus duration of implantation; $p<0.001$ (two-way ANOVA); #$p<0.05$ (Mann–Whitney test) for the BG constructs compared with the other two material constructs. (E) hBMSC, still present in the constructs explanted 2 months postimplantation, were detected on paraffin-treated sections following immunostaining against human β-2-microglobulin. *Scaffold material (either HA/TCP, coral, or BG); black arrow head indicates cells stained positive for human β-2-microglobulin. BLI, bioluminescent. Color images available online at www.liebertpub.com/tea

Cell viability was also assessed by determining hBMSC proliferation within 3D cell-containing constructs composed of either HA/TCP, coral, or BG granules embedded in the fibrin gel (Fig. 3C). Proliferation of hBMSC (previously labeled with the luciferase gene reporter) was monitored nondestructively in each construct using bioluminescence imaging. Similar profiles of LuchBMSC proliferation kinetics were observed for the three types of constructs of interest to the present study. Compared with the initial seeding, the number of cells increased by 2- to 3-fold after 15 days of culture; the highest cell proliferation was observed in the BG constructs (3.4-fold at day 14; $p<0.05$ compared with the other two material constructs) (Fig. 3C). Furthermore, hBMSC survival was also assessed in vivo after subcutaneous implantation of the cell-containing constructs in nude mice for 2 months (Fig. 3D). For the cases tested, the number of viable implanted cells decreased over this time period. The decrease in cell survival was significantly ($p<0.05$) slower in the BG constructs compared with that obtained on the HA/TCP and coral ones up to 14 days postimplantation. After that time point, a steady decrease in the luminescence signal from all implanted cell-containing constructs was observed (Fig. 3D). As a result, only 10% to 30% of the initial cell numbers remained for all constructs tested at 8 weeks postimplantation. These results indicated a loss of viable hBMSC, which occurred upon implantation independent of the type of material tested; more importantly, the implanted hBMSC did not die faster in the BG than in the other two material constructs.

Immunostaining of human β-2-microglobulin enabled visualization of the hBMSC still present in sections of constructs explanted 8 weeks postimplantation (Fig. 3E). Human β-2-microglobulin-positive cells were detected at different locations in the tissue surrounding the granules, but were most frequently found on the material surface of all three types of constructs tested (Fig. 3E). These results confirmed the cytocompatibility of the three materials tested over the 8-week period of implantation. It should be noted that hBMSC were detected not only in fibroblastic connective tissue, but also in newly formed bone as well as around blood vessels in the HA/TCP- and coral-cell-containing constructs (data not shown). In contrast, positive-stained hBMSC were only detected in the fibroblastic connective tissue in the BG-cell-containing constructs. Overall, cell spreading on the granule surfaces (Fig. 3A), cell proliferation in vitro (Fig. 3B, C), as well as the scaffold material cytocompatibility in vivo (Fig. 3D, E) provided evidence that the observed absence of de novo bone formation in the hBMSC-containing BG constructs is not the result of lack of cytocompatibility of the BG material.

Osteogenic differentiation of hBMSC cultured onto the materials tested

Another aspect addressed in the present study was the potential for osteogenic differentiation of hBMSC cultured on BG granules as compared with results obtained on either the HA/TCP or coral

substrates. For this purpose, the ALP activity of hBMSC cultured in the osteogenic differentiation medium on the three material granules tested was assessed. The ALP activity of hBMSC cultured on either HA/TCP or coral granules peaked at 14 days (Fig. 4A), indicating osteogenic differentiation of hBMSC on these materials. HBMSC exhibited a significantly ($p<0.05$) greater ALP activity on HA/TCP and coral than on BG granules at 14 and 21 days of culture (Fig. 4A). In addition, the ALP activity of hBMSC cultured on TCPS (reference substrate) was three-, three-, and sevenfold higher than that obtained when the cells were cultured onto the HA/TCP, coral, and BG granules, respectively (data not shown). The results were confirmed by the enhanced positive ALP staining of cells cultured on HA/TCP and on coral granules compared with BG ones for 14 and 28 days (Fig. 4B).

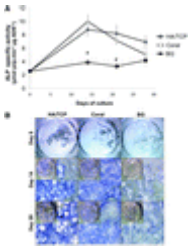

FIG. 4. Osteogenic differentiation of hBMSC cultured onto granules of HA/TCP, coral, and BG. (A) Kinetics of the ALP activity expressed by hBMSC; $p<0.001$ (two-way ANOVA) and #$p<0.05$ (Mann–Whitney test) compared with values obtained with either HA/TCP or coral granules at the same time point. (B) hBMSC stained in situ for ALP after 0, 14, and 28 days of cell culture. ALP, alkaline phosphatase. Color images available online at www.liebertpub.com/tea

A panel of genes indicative of osteogenic differentiation was also investigated using quantitative polymerase chain reaction (qPCR) (Supplementary Fig. S1; Supplementary Data are available online at www.liebertpub.com/tea). Expressions of all markers (specifically, RUNX2, Osterix, Col1a1, OC, and OPN) tested by hBMSC were similar when cultured on the three types of granules at both 7 and 14 days of culture.

Determination of the pH in the material constructs tested

The pH in the core environment of the cell-free BG constructs was determined to assess the alkalinization induced by the material itself (in the absence of cell-mediated acidosis). Starting from 7.4, the pH increased during the first hours postgelation and reached a plateau at later (>10 h) times (Fig. 5A). At 24 h postgelation, the pH values in the HA/TCP-, coral-, and BG-containing constructs were 8.6, 8.3, and 9.1±0.1, respectively. The pH of the BG constructs was 0.5 and 0.8 U more alkaline than the pH determined in the HA/TCP and coral constructs, respectively.

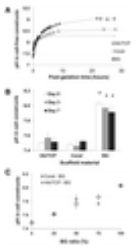

FIG. 5. pH determination within the material constructs. (A) Time course of pH values at the core of the material granule constructs (without cells) using a microelectrode inserted before fibrin gelation. (B) pH measurements from cell constructs before (day 0) and after in vivo subcutaneous implantation

for either 3 or 7 days. (C) In vitro pH determination as a function of the ratio (from 0% to 100% in weight) of BG granules in either HA/TCP: BG or coral: BG cell-containing composite constructs. #p<0.05 (Mann–Whitney test) compared with values obtained with either HA/TCP or coral materials at the same time point.

Because these cell-free conditions did not reflect those of the cell-containing constructs implanted in vivo, the pH of constructs seeded with 106 cells was also measured before their implantation (day 0) and immediately upon their removal from mice after 3 and 7 days of implantation. The pH in the cell-containing BG constructs was 8.03±0.03 at day 0 and remained similar at the prescribed postimplantation time points (Fig. 5B). The pH value in these BG constructs was 0.4–0.5 U more alkaline ($p<0.05$) than that measured in the other two types of cell-containing material constructs. The pH from both cell-containing HA/TCP:BG and coral:BG composite constructs that contained increasing ratios of BG was also measured in vitro. The data showed a strong correlation ($r2=0.88$ and 0.99 for the HA/TCP:BG and the coral: BG composites, respectively) between the pH and the content of BG in the scaffolds of cell-containing constructs (Fig. 5C). Altogether, these results confirmed the alkalinization of the environment of the BG cell-containing constructs.

Osteogenic differentiation of hBMSC as a function of the pH of the cell culture medium

The effect of the pH of the cell culture medium (ranging from 7.47 to 9.37 using the HEPES buffer) on both the proliferation and the osteoblastic differentiation potential of hBMSC was also investigated. It is worth noting that a decrease of both pHini and pHfin values ranging from 0.1 U of pH, for the lowest pHini (7.47), to 0.8 U for the highest pHini (9.37) value was noticed after 2–3 days of cell culture (Table in Fig. 6D).

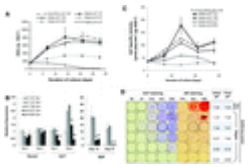

FIG. 6. Osteogenic differentiation of hBMSC as a function of the pH of the culture medium. (A) Proliferation of hBMSC cultured in buffered osteogenic medium either using a standard CO2/HCO3 system or adjusted to increasing alkaline pH values using 25 mM HEPES; $p<0.001$ (two-way ANOVA) for the cell cultures at either pH 8.85 or 9.37; these results were compared with those obtained from cell cultures at other pH values (specifically, 7.47, 7.54, 7.90, and 8.27). (B) Gene expression of RUNX2, ALP, and BSP by hBMSC cultured in osteogenic medium (Os+); gene expression was normalized first to that of the respective 18S (internal standard), and then to results obtained when cells were cultured in the nonosteogenic culture medium (Os−); $ap<0.05$ compared with pH 7.47 Os+ group; $bp<0.05$ compared with pH 7.90 Os+ group; $cp<0.05$ compared with pH 8.27 Os+ group (Mann–Whitney tests). (C) Kinetics of the ALP activity expressed by hBMSC cultured in osteogenic medium; $p<0.001$ (two-way ANOVA) for the cell cultures performed at either pH 8.27 or 8.85 compared with cultures at other pH (specifically, 7.47, 7.54, and 7.90). (D) ALP and Alizarin red (AR) in situ stainings of hBMSC. Average values of both the initial and final pH of the supernatant culture medium, which were determined at each medium change during the course of the experiment, are indicated in the Table included on this frame. BSP, bone sialoprotein; HEPES, 4-(2-hydroxyethyl)-1-piperazineethanesulfonic acid; RUNX2, runt-related transcription factor 2. Color images available online at www.liebertpub.com/tea

Under these conditions, DNA quantification provided evidence that hBMSC proliferation was unaffected at alkaline pH up to 8.27; there was no cell proliferation at pH 8.85 and the cells died at pH 9.37 (Fig. 6A). To assess the impact of the medium pH on the osteoblastic differentiation potential of hBMSC, a panel of genes indicative of osteogenic differentiation was investigated using qPCR (Fig. 6B). hBMSC were cultured in the nonosteogenic medium as negative control. At either physiological pHini (7.47) or moderate alkaline pHini (≤7.90), expression of the osteoblastic (RUNX2, ALP, and BSP) markers was higher when the cells were cultured in osteogenic than in nonosteogenic media indicating osteogenic differentiation of the hBMSC in the range of these pH values (7.47≤pHini≤7.90). At higher (>7.90) pHini, gene expression of the three markers monitored dramatically decreased and reached similar, or even lower, levels of expression as the ones obtained when the cells were cultured in the nonosteogenic medium.

The extent of both the ALP activity and mineralization of the hBMSC ECM was also strongly dependent on the pH of the cell culture medium (Fig. 6C, D). The highest level of ALP activity occurred at day 14 when the cells were cultured at pHini 7.47 (Fig. 6C). Similar results were obtained when the cell culture medium was buffered (using a CO2/HCO3 system) either at pHini 7.54 or at a moderate alkaline pHini (7.90) level (Fig. 6C). At pHini 8.27, the ALP activity significantly decreased, while at pHini 8.85, minimal ALP production occurred at a later time, specifically, at 28 days of culture (Fig. 6C). ALP staining of cells confirmed these results (Fig. 6D). Mineralization of the hBMSC ECM occurred only at physiologic pHini (pHini<7.54) and was visualized using AR staining (Fig. 6D). It is worth noting, however, that the cell culture medium buffered with HEPES affected the mineralization process; at similar pHini, the kinetics of mineral accumulation was delayed and the amount of mineral deposited was lower in the HEPES-buffered system compared with the results obtained using the CO2/HCO3 system (Fig. 6D).

These results provided evidence that the alkaline pH (specifically, pH>7.9) affected adversely both the hBMSC osteogenic differentiation and, more strongly, the mineralization process of the ECM. Interestingly, while hBMSC proliferation (Fig. 6A) was not affected at pH 8.27 (the pH value in the vicinity of the BG granules in the cell constructs tested), their osteogenic differentiation was inhibited (Fig. 6B, C).

Discussion

The present study is the first to address the impact of pH in the microenvironment of bone TE constructs on osteogenesis. The results provided evidence that constructs of hBMSC contained in a material, specifically, BG, induces alkalinization of the microenvironment did not promote de novo bone formation; in contrast, cell-containing constructs prepared with either HA/TCP or coral, the two other materials tested, did not change significantly the microenvironment pH, but consistently induced bone tissue.

BG is well known to alkalinize surrounding fluids22,23 due to the consumption of protons (H3O+ ions) during the ion exchange reactions between the glass network and the aqueous media.41 In the present study, the pH within the cell-free BG constructs was around 9.0 and decreased to 8.0 in the cell-containing BG constructs both before and after implantation in mice. This decrease in pH value, although without reaching the physiological value (7.4), is explained by the acidosis that accompanies cell metabolism. In addition, the strong correlation established between the pH and the proportion (in weight) of BG granules within the cell-containing composite constructs confirmed the effect of BG material in the alkalization process.

The hBMSC-mediated osteogenic potential was assessed in vivo after subcutaneous implantation of the cell-containing material constructs in mice. This is a standard in vivo model that excludes and/or reduces the effects of endogenous bone-forming cells and of bone-stimulating mechanotransduction on the process of new bone formation.13,42 Interestingly, the in vivo results evidenced that the implanted 50:50 composites of both HA/TCP:BG and coral:BG constructs, whose pH was around 7.8, had very little amount of bone tissue after 8 weeks postimplantation. Altogether, these results evidenced a correlation between loss of the bone forming potential of the cell-containing constructs and the degree of alkalinization within these constructs: osteogenesis decreased 20–30-fold when the pH rose from 7.5 to 7.8, and it was totally inhibited when the pH reached 8.

BG and glass ceramics are widely used in bone repair applications and are considered appropriate materials for bone TE applications.43 However, information regarding the performance of BG as scaffolds for the delivery of osteocompetent cells in TE applications has been lacking. The absence of osteoinductivity observed with BG-containing constructs in the present study is in agreement with the results from other groups who reported that various formulations of silicate glasses (such as 45S5 BG, 13–93 BG, and BG/polymer composites) seeded with stem/precursor cells promoted abundant fibrous tissue infiltration upon implantation in ectopic sites in rodents. These studies reported the presence of sporadic osteoid or bone-like tissue within constructs, but none of them evidenced bone tissue formation unequivocally.44–46

In the present study, histological analysis of the composite constructs tested showed that the bone tissue was located onto the surface of either HA/TCP or coral, but not on BG. Such observation suggests that the reduced osteogenic potential in BG-containing constructs in vivo was closely related to the BG material surface and/or to its local microenvironment.

In respect to the physical properties of the material surface, the SEM images showed that, at the scale of hBMSC, that is, 20–50 μm, the topography, roughness, and available material surface for cell attachment were equivalent for the three materials tested. In respect to the material microenvironment, it is well documented that dissolution of BG material mediates the release of ions such as Na+, Ca2+, and Si products (presumably in the form of silicic acid Si(OH)4) into the surrounding aqueous media; continuous hydrolysis of silica groups results in increased local pH.19

The impact of both material surface physicochemistry and dissolution products (released in the microenvironment) on the hBMSC cytocompatibility was evaluated in vitro and in vivo. In vitro, both adhesion and proliferation of hBMSC cultured directly onto the BG surface were not affected compared with the other materials tested. When hBMSC were seeded within 3D BG constructs, and, therefore, exposed locally to this material dissolution product, cell viability was even higher compared with respective results obtained from the other two types of material constructs tested both in vitro and in vivo. Implanted hBMSC still remained on the surface of all types of materials tested 8 weeks postimplantation.

Among the hypotheses that could explain the observed higher viability of hBMSC in BG constructs is the possible impact of BG on the metabolic activity of cells. Indeed, Silver et al. reported that BG enhanced glycolysis in osteoblasts in vitro and, thus, their cellular ATP production; those authors stated that these metabolic effects are most likely consequences of external and internal alkalinization in the cell milieu.22 If BG has similar effects on the hBMSC metabolism in vivo, as it does on osteoblasts in vitro,22 stimulation of ATP generation may be beneficial for cell viability inside the TE constructs tested. All in all, these data confirmed that BG materials are cytocompatible both in vitro and in vivo in agreement with previous studies.47,48

On one hand, viability of hBMSC was not affected by BG, on the other hand, however, its potential for osteogenic differentiation was diminished in vitro. Such result obtained in vitro, as well as lack of osteogenic evidence in the cell-containing BG constructs in vivo, seems to be affected by the ionic exchange occurring at the surface of the material and/or by its side effects (such as pH changes). This hypothesis is strengthened by the minimal bone formation obtained from the 50:50 composites of both HA/TCP:BG and coral:BG constructs: osteogenesis decreased 20–30-fold when half (in weight) of either the HA/TCP or coral granules was replaced by BG granules; this result suggests that one or several diffusible chemicals, such as ion complexes (concomitant to pH changes), impede the hBMSC-mediated osteogenesis.

The aforementioned results are in striking contrast with the numerous literature reports regarding the beneficial effects of products released from BG (without taking into account concomitant pH changes) on various functions (such as proliferation, differentiation, ECM production, mineralization, and even angiogenesis) of human progenitors pertinent to new tissue formation.49–52 Especially, Si products were reported to enhance osteogenic markers in osteoprogenitor cells.53,54 Nevertheless, within the microenvironment of the BG constructs in vivo, cells may have been exposed locally to higher concentrations of Si products in the present study than those used in the published studies. Thus, one cannot exclude that release of ions/species (such as Na+, Ca2+, or more particularly Si(OH)4) from the BG granules into their microenvironment in the present study, may have contributed to the inhibition of bone tissue formation in vivo.

The release of Si products from the BG material and the subsequent alkalinization of the surrounding medium are two chemical events that could not be separated in the present study because they are closely interlinked.19 However, the observed considerable (0.5 U) rise in the pH of the BG constructs (compared with the other two types of material constructs tested) raised questions regarding how the biological, in particular osteogenic, responses of hBMSC were affected in an alkaline milieu. It should be noted that alkalinization of the external medium was likely accompanied by a shift in the intracellular pH (pHint) in the same direction. However, the magnitude of change in the pHint is usually smaller than that in the external/extracellular pH (pHext) because of the control mechanisms (such as ion-transport systems) in eukaryotic cells.22,55

The present results provided evidence that the in vitro hBMSC proliferation and osteogenic differentiation were not significantly affected at moderate alkaline pHext (up to 7.90), but were dramatically inhibited when the pHext increased further. Formation of mineralized nodules in the ECM of hBMSC proved more sensitive to the pHext since it was fully inhibited at alkaline (>7.54) pHext values. Most importantly, these findings indicated that there is a pHext range (specifically, 7.9–8.27) at which hBMSC proliferation was not affected, but the osteogenic differentiation of these cells was inhibited. Such pHext range encompassed the one determined in the cell-containing BG granules (pHext ∼8) and could not only explain the observed proliferation of hBMSC in BG constructs in vitro and the cell viability in vivo, but also the absence of bone tissue formation in vivo.

The effect of the pH of the tissue microenvironment on bone mineralization and repair has been reported previously.56–58 During the early healing phase in bone, Chakkalakal et al. determined that the tissue pH was lower than the physiologic (7.4) pH; when subsequently this pH increased to more alkaline values (specifically, to pH 7.56), it was accompanied by mineral deposition.25 On a cellular level, during metabolic acidosis, osteoblast functions decline, whereas during metabolic alkalosis, osteoblast functions (specifically, cell viability, ALP activity, and mineral deposition) increase.10,26–28 With respect to bone TE using hBMSC, Kohn et al. reported that short-term (specifically, 48 h) exposure of hBMSC at decreasing (specifically, from 7.8 to ≤6.5) pH led to the decrease of osteogenic phenotype markers, specifically, ALP activity and collagen synthesis.59 Some of the aforementioned

studies, however, reported a decrease of the osteoblastic activity at pH around 7.8,27,60 but have not tested a pH range that encompasses the excessive alkalosis (pH ~8) observed in the microenvironment of the cell-containing BG constructs tested in the present study. Therefore, it is possible that the high local alkalinization induced by the BG constructs had adverse effects on the osteogenic differentiation of stem cells in contrast to the beneficial effects obtained with moderate alkalosis; in fact, such a condition was deleterious to hBMSC metabolism and function in vitro and, therefore, likely to their bone formation ability in vivo.

In conclusion, the results of the present study evidenced a close relationship between inhibition of the hBMSC-mediated osteogenesis observed in vivo and the local alkalinization within the TE constructs tested. Excessive alkalinization in the TE construct microenvironment (resulting, for example, from material degradation) affected adversely the osteogenic differentiation of osteoprogenitor cells and may have consequently inhibited the osteogenicity of the constructs in vivo. Thorough characterization and control of the local, engineered, extracellular environment (specifically, changes of pH) are critical issues, which must be addressed in the development of bioactive scaffolds for successful TE, bone-related applications.

Acknowledgments

The authors gratefully acknowledge Inoteb, Inc. (Levallois- Perret, France) for donating the coral scaffolds and Baxter, Inc., for donating the Tissucol used in the present study. The authors are grateful to Brigitte Gaillard (INRA, Unité de Microbiologie, Clermont-Ferrand, France) for conducting the SEM analysis for cell adhesion. The authors also thank Professor R. Bizios for critically reading the article. This project was supported by the French National Research Agency (ANR) through the TecSan program (project GLASSBONE no. 08-TECS-004), and by the Centre National de la Recherche Scientifique (CNRS) of France.

Disclosure Statement

The authors declare no competing financial interests.

References

1. A.J. Friedenstein, R.K. Chailakhyan, and U.V. Gerasimov Bone marrow osteogenic stem cells: in vitro cultivation and transplantation in diffusion chambers. Cell Tissue Kinet 20, 263, 1987.

2. J. Goshima, V.M. Goldberg, and A.I. Caplan Osteogenic potential of culture-expanded rat marrow cells as assayed in vivo with porous calcium phosphate ceramic. Biomaterials 12, 253, 1991.

3. S.P. Bruder, N. Jaiswal, N.S. Ricalton, J.D. Mosca, K.H. Kraus, and S. Kadiyala Mesenchymal stem cells in osteobiology and applied bone regeneration. Clin Orthop Relat Res S247, 1998.

4. H. Petite, V. Viateau, W. Bensaid, A. Meunier, C. de Pollak, M. Bourguignon, et al. Tissue-engineered bone regeneration. Nat Biotechnol 18, 959, 2000.

5. E. Kon, A. Muraglia, A. Corsi, P. Bianco, M. Marcacci, I. Martin, et al. Autologous bone marrow stromal cells loaded onto porous hydroxyapatite ceramic accelerate bone repair in critical-size defects of sheep long bones. J Biomed Mater Res 49, 328, 2000.

6. R. Quarto, M. Mastrogiacomo, R. Cancedda, S.M. Kutepov, V. Mukhachev, A. Lavroukov, et al. Repair of large bone defects with the use of autologous bone marrow stromal cells. N Engl J Med 344, 385, 2001.

7. C.M. Agrawal, and R.B. Ray Biodegradable polymeric scaffolds for musculoskeletal tissue engineering. J Biomed Mater Res 55, 141, 2001.

8. F.J. O'Brien, B.A. Harley, I.V. Yannas, and L.J. Gibson The effect of pore size on cell adhesion in collagen-GAG scaffolds. Biomaterials 26, 433, 2005.

9. H. Chang, and Y. Wang Cell responses to surface and architecture of tissue engineering scaffolds. In: D. Eberli, ed. Regenerative Medicine and Tissue Engineering—Cells and Biomaterials. Intech, 2011. http://www.intechopen.com/books/regenerative-medicine-and-tissue-engineering-cells-and-biomaterials/cell-responses-to-surface-and-architecture-of-tissue-engineering-scaffolds. ISBN: 978-953-307-663-8.

10. Y. Shen, W. Liu, C. Wen, H. Pan, T. Wang, B.W. Darvell, et al. Bone regeneration: importance of local pH—strontium-doped borosilicate scaffold. J Mater Chem 22, 8662, 2012.

11. A. El-Ghannam Bone reconstruction: from bioceramics to tissue engineering. Expert Rev Med Devices 2, 87, 2005.

12. R.Z. LeGeros Calcium phosphate-based osteoinductive materials. Chem Rev 108, 4742, 2008.

13. P.H. Krebsbach, S.A. Kuznetsov, K. Satomura, R.V. Emmons, D.W. Rowe, and P.G. Robey Bone formation in vivo: comparison of osteogenesis by transplanted mouse and human marrow stromal fibroblasts. Transplantation 63, 1059, 1997.

14. M.H. Mankani, S.A. Kuznetsov, and P.G. Robey Formation of hematopoietic territories and bone by transplanted human bone marrow stromal cells requires a critical cell density. Exp Hematol 35, 995, 2007.

15. A.C. Zannettino, S. Paton, S. Itescu, and S. Gronthos Comparative assessment of the osteoconductive properties of different biomaterials in vivo seeded with human or ovine mesenchymal stem/stromal cells. Tissue Eng Part A 16, 3579, 2010.

16. T.L. Arinzeh, T. Tran, J. McAlary, and G. Daculsi A comparative study of biphasic calcium phosphate ceramics for human mesenchymal stem-cell-induced bone formation. Biomaterials 26, 3631, 2005.

17. T. Cordonnier, P. Layrolle, J. Gaillard, A. Langonne, L. Sensebe, P. Rosset, et al. 3D environment on human mesenchymal stem cells differentiation for bone tissue engineering. J Mater Sci Mater Med 21, 981, 2010.

18. M. Sladkova, M. Manassero, V. Myrtil, H. Savari, M. Fall, D. Thomas, et al. Coral particle size influences human mesenchymal stem cell osteogenesis but not cell survival in an ectopic mouse model. European Orthopaedic Research Society, Amsterdam, 2012.

19. M.N. Rahaman, D.E. Day, B.S. Bal, Q. Fu, S.B. Jung, L.F. Bonewald, et al. Bioactive glass in tissue engineering. Acta Biomater 7, 2355, 2011.

20. L.L. Hench, and J.M. Polak Third-generation biomedical materials. Science 295, 1014, 2002.

21. A. el-Ghannam, P. Ducheyne, and I.M. Shapiro Formation of surface reaction products on bioactive glass and their effects on the expression of the osteoblastic phenotype and the deposition of mineralized extracellular matrix. Biomaterials 18, 295, 1997.

22. I.A. Silver, J. Deas, and M. Erecinska Interactions of bioactive glasses with osteoblasts in vitro: effects of 45S5 Bioglass, and 58S and 77S bioactive glasses on metabolism, intracellular ion concentrations and cell viability. Biomaterials 22, 175, 2001.

23. D. Zhang, M. Hupa, and L. Hupa In situ pH within particle beds of bioactive glasses. Acta Biomater 4, 1498, 2008.

24. W.B. Busa, and R. Nuccitelli Metabolic regulation via intracellular pH. Am J Physiol 246, R409, 1984.

25. D.A. Chakkalakal, A.A. Mashoof, J. Novak, B.S. Strates, and M.H. McGuire Mineralization and pH relationships in healing skeletal defects grafted with demineralized bone matrix. J Biomed Mater Res 28, 1439, 1994.

26. D.A. Bushinsky Metabolic alkalosis decreases bone calcium efflux by suppressing osteoclasts and stimulating osteoblasts. Am J Physiol 271, F216, 1996.

27. A. Brandao-Burch, J.C. Utting, I.R. Orriss, and T.R. Arnett Acidosis inhibits bone formation by osteoblasts in vitro by preventing mineralization. Calcif Tissue Int 77, 167, 2005.

28. T.R. Arnett Acidosis, hypoxia and bone. Arch Biochem Biophys 503, 103, 2010.

29. G. Guillemin, A. Meunier, P. Dallant, P. Christel, J.C. Pouliquen, and L. Sedel Comparison of coral resorption and bone apposition with two natural corals of different porosities. J Biomed Mater Res 23, 765, 1989.

30. G. Guillemin, J.L. Patat, J. Fournie, and M. Chetail The use of coral as a bone graft substitute. J Biomed Mater Res 21, 557, 1987.

31. L.L. Hench Bioactive materials: the potential for tissue regeneration. J Biomed Mater Res 41, 511, 1998.

32. T. Kokubo, H. Kushitani, S. Sakka, T. Kitsugi, and T. Yamamuro Solutions able to reproduce in vivo surface-structure changes in bioactive glass-ceramic A-W. J Biomed Mater Res 24, 721, 1990.

33. T. Kokubo, and H. Takadama How useful is SBF in predicting in vivo bone bioactivity? Biomaterials 27, 2907, 2006.

34. M. Mačković, A. Hoppe, R. Detsch, D. Mohn, W.J. Stark, E. Spiecker, et al. Bioactive glass (type 45S5) nanoparticles: in vitro reactivity on nanoscale and biocompatibility. J Nanopart Res 14, 966, 2012.

35. D. Marchat, D. Bernache-Assollant, and E. Champion Cadmium fixation by synthetic hydroxyapatite in aqueous solution—thermal behaviour. J Hazard Mater 139, 453, 2007.

36. P. Becquart, A. Cambon-Binder, L.E. Monfoulet, M. Bourguignon, K. Vandamme, M. Bensidhoum, et al. Ischemia is the prime but not the only cause of human multipotent stromal cell death in tissue-engineered constructs in vivo. Tissue Eng Part A 18, 2084, 2012.

37. W. Bensaid, J.T. Triffitt, C. Blanchat, K. Oudina, L. Sedel, and H. Petite A biodegradable fibrin scaffold for mesenchymal stem cell transplantation. Biomaterials 24, 2497, 2003.

38. D. Logeart-Avramoglou, K. Oudina, M. Bourguignon, L. Delpierre, M.A. Nicola, M. Bensidhoum, et al. In vitro and in vivo bioluminescent quantification of viable stem cells in engineered constructs. Tissue Eng Part C Methods 16, 447, 2010.

39. M.C. Degat, G. Dubreucq, A. Meunier, L. Dahri-Correia, L. Sedel, H. Petite, et al. Enhancement of the biological activity of BMP-2 by synthetic dextran derivatives. J Biomed Mater Res Part A 88, 174, 2009.

40. K. Vandamme, X. Holy, M. Bensidhoum, D. Logeart-Avramoglou, I. Naert, J. Duyck, et al. Establishment of an in vivo model for molecular assessment of titanium implant osseointegration in compromised bone. Tissue Eng Part C Methods 17, 311, 2011.

41. L.L. Hench Bioceramics. J Am Ceram Soc 81, 1705, 1998.

42. M.H. Mankani, S.A. Kuznetsov, N.A. Avila, A. Kingman, and P.G. Robey Bone formation in transplants of human bone marrow stromal cells and hydroxyapatite-tricalcium phosphate: prediction with quantitative CT in mice. Radiology 230, 369, 2004.

43. P. Ducheyne, and Q. Qiu Bioactive ceramics: the effect of surface reactivity on bone formation and bone cell function. Biomaterials 20, 2287, 1999.

44. R. El-Gendy, X.B. Yang, P.J. Newby, A.R. Boccaccini, and J. Kirkham Osteogenic differentiation of human dental pulp stromal cells on 45S5 Bioglass(R) based scaffolds in vitro and in vivo. Tissue Eng Part A 19, 707, 2013.

45. Q. Fu, M.N. Rahaman, B.S. Bal, L.F. Bonewald, K. Kuroki, and R.F. Brown Silicate, borosilicate, and borate bioactive glass scaffolds with controllable degradation rate for bone tissue engineering applications. II. In vitro and in vivo biological evaluation. J Biomed Mater Res Part A 95, 172, 2010.

46. V.S. Gomide, A. Zonari, N.M. Ocarino, A.M. Goes, R. Serakides, and M.M. Pereira In vitro and in vivo osteogenic potential of bioactive glass-PVA hybrid scaffolds colonized by mesenchymal stem cells. Biomed Mater 7, 015004. 2012.

47. J. Wilson, G.H. Pigott, F.J. Schoen, and L.L. Hench Toxicology and biocompatibility of bioglasses. J Biomed Mater Res 15, 805, 1981.

48. M. Bosetti, L. Zanardi, L. Hench, and M. Cannas Type I collagen production by osteoblast-like cells cultured in contact with different bioactive glasses. J Biomed Mater Res Part A 64, 189, 2003.

49. I.D. Xynos, A.J. Edgar, L.D. Buttery, L.L. Hench, and J.M. Polak Gene-expression profiling of human osteoblasts following treatment with the ionic products of Bioglass 45S5 dissolution. J Biomed Mater Res 55, 151, 2001.

50. O. Tsigkou, J.R. Jones, J.M. Polak, and M.M. Stevens Differentiation of fetal osteoblasts and formation of mineralized bone nodules by 45S5 Bioglass conditioned medium in the absence of osteogenic supplements. Biomaterials 30, 3542, 2009.

51. R.M. Day Bioactive glass stimulates the secretion of angiogenic growth factors and angiogenesis in vitro. Tissue Eng 11, 768, 2005.

52. A. Leu, and J.K. Leach Proangiogenic potential of a collagen/bioactive glass substrate. Pharm Res 25, 1222, 2008.

53. P. Han, C. Wu, and Y. Xiao The effect of silicate ions on proliferation, osteogenic differentiation and cell signalling pathways (WNT and SHH) of bone marrow stromal cells. Biomater Sci 1, 379, 2013.

54. D.M. Reffitt, N. Ogston, R. Jugdaohsingh, H.F. Cheung, B.A. Evans, R.P. Thompson, et al. Orthosilicic acid stimulates collagen type 1 synthesis and osteoblastic differentiation in human osteoblast-like cells in vitro. Bone 32, 127, 2003.

55. C. Frelin, P. Vigne, A. Ladoux, and M. Lazdunski The regulation of the intracellular pH in cells from vertebrates. Eur J Biochem 174, 3, 1988.

56. O. Swenson, and C.L. Claff Changes in the hydrogen ion concentration of healing fractures. Proc Soc Exp Biol Med 61, 151, 1946.

57. T.R. Arnett, and D.W. Dempster Effect of pH on bone resorption by rat osteoclasts in vitro. Endocrinology 119, 119, 1986.

58. R.J. Newman, M.J. Francis, and R.B. Duthie Nuclear magnetic resonance studies of experimentally induced delayed fracture union. Clin Orthop Relat Res 216, 253, 1987.

59. D.H. Kohn, M. Sarmadi, J.I. Helman, and P.H. Krebsbach Effects of pH on human bone marrow stromal cells in vitro: implications for tissue engineering of bone. J Biomed Mater Res 60, 292, 2002.

60. K.K. Kaysinger, and W.K. Ramp Extracellular pH modulates the activity of cultured human osteoblasts. J Cell Biochem 68, 83, 1998.